

Spatiotemporal structure of visual receptive fields in macaque superior colliculus

Jan Churan, Daniel Guitton, and Christopher C. Pack

Montreal Neurological Institute, McGill University, Montreal, Quebec, Canada

Submitted 9 May 2012; accepted in final form 24 August 2012

Churan J, Guitton D, Pack CC. Spatiotemporal structure of visual receptive fields in macaque superior colliculus. *J Neurophysiol* 108: 2653–2667, 2012. First published August 29, 2012; doi:10.1152/jn.00389.2012.—Saccades are useful for directing the high-acuity fovea to visual targets that are of behavioral relevance. The selection of visual targets for eye movements involves the superior colliculus (SC), where many neurons respond to visual stimuli. Many of these neurons are also activated before and during saccades of specific directions and amplitudes. Although the role of the SC in controlling eye movements has been thoroughly examined, far less is known about the nature of the visual responses in this area. We have, therefore, recorded from neurons in the intermediate layers of the macaque SC, while using a sparse-noise mapping procedure to obtain a detailed characterization of the spatiotemporal structure of visual receptive fields. We find that SC responses to flashed visual stimuli start roughly 50 ms after the onset of the stimulus and last for on average ~70 ms. About 50% of these neurons are strongly suppressed by visual stimuli flashed at certain locations flanking the excitatory center, and the spatiotemporal pattern of suppression exerts a predictable influence on the timing of saccades. This suppression may, therefore, contribute to the filtering of distractor stimuli during target selection. We also find that saccades affect the processing of visual stimuli by SC neurons in a manner that is quite similar to the saccadic suppression and postsaccadic enhancement that has been observed in the cortex and in perception. However, in contrast to what has been observed in the cortex, decreased visual sensitivity was generally associated with increased firing rates, while increased sensitivity was associated with decreased firing rates. Overall, these results suggest that the processing of visual stimuli by SC receptive fields can influence oculomotor behavior and that oculomotor signals originating in the SC can shape perisaccadic visual perception.

superior colliculus; visuomotor integration; macaque

IN HUMANS AND OTHER primates, high-acuity vision results from a small, central region of the retina known as the fovea. Outside of this region, acuity decreases sharply, and consequently the primate brain has evolved mechanisms for rapidly and accurately pointing the fovea at objects of interest in the environment. These mechanisms involve saccadic eye movements that are typically executed several times per second.

The oculomotor system informs other brain areas about impending eye movements using a mechanism called an efference copy (von Holst and Mittelstedt 1950) or a corollary discharge (Sperry 1950). As a consequence, the visual system changes its response properties around the time of saccades in different ways (for a review, see Sommer and Wurtz 2008; Wurtz 2008). Similarly, visual perception exhibits a variety of changes around the time of each saccade, including changes in

overall visual sensitivity (Burr et al. 1999), motion perception (Lee and Lee 2005), and the perception of visual space (Lappe et al. 2000; Richard et al. 2009; Ross et al. 1997; van Wetter and van Opstal 2008). Correlates of these perceptual effects have been found at the single-neuron level in various brain regions (Bremmer et al. 2009; Ibbotson et al. 2008; Ilg and Hoffmann 1993). Thus information about eye movements and visual stimuli are combined in many brain regions, and this integration exerts a powerful influence on perception.

A particularly clear example of the integration of visual and oculomotor information occurs in the intermediate and deep layers of the superior colliculus (SC), where individual neurons encode both the metrics of an impending saccade and the location of visual stimuli (Wurtz and Goldberg 1971, 1972). The substantial overlap between the spatial encoding of these two quantities (Marino et al. 2008; Wurtz and Goldberg 1972) suggests a role for the SC in the selection of saccade targets. This role has been confirmed experimentally through microstimulation (Dorris et al. 2007; Guitton et al. 1980; McPeck et al. 2003) and inactivation (McPeck and Keller 2004; McPeck 2008; Nummela and Krauzlis 2010).

If visual receptive fields (RFs) in the SC are involved in target selection, one might expect that the specific structure of the RFs should be predictive of the timing and accuracy of saccades. In particular, in cluttered visual scenes, the precise arrangement of potential distractors should affect saccades in a way that depends on the shape of visual RFs (Dorris et al. 2007; Edelman and Xu 2009). Although previous work has provided important information about the general visual properties of SC RFs, including their stimulus selectivity (Cynader and Berman 1972; Marrocco and Li 1977; Updyke 1974), their shape and size (Cynader and Berman 1972; Humphrey 1968; Marino et al. 2008; Wurtz and Goldberg 1972), their adaptation properties (Humphrey 1968; Marrocco and Li 1977), and the strength and distribution of suppressive surrounds (Cynader and Berman 1972; Updyke 1974), a quantitative estimate of the detailed spatiotemporal structure of the RFs has not been obtained.

Sparse noise mapping is a procedure that is widely used to recover the spatial and temporal structure of visual RFs (Jones and Palmer 1987; Livingstone et al. 2001; Pack et al. 2006; Ringach and Shapley 2004; Szulborski and Palmer 1990). In this work, we have used a sparse noise-mapping procedure to characterize visual RFs in the intermediate and deep layers of SC of the macaque monkey. Specifically, we have stimulated SC neurons with random patterns of visual stimuli while the animals alternated between periods of fixation and saccades. The subsequent analysis provided a detailed picture of the spatial and temporal structure of SC RFs, allowing us to

Address for reprint requests and other correspondence: J. Churan, Montreal Neurological Institute, 3801 Univ. St., #896, Montreal, Quebec, Canada H3A 2B4 (e-mail: jan.churan@gmail.com).

recover the structure and the time dependence of excitatory and suppressive influences on each SC neuron. The suppressive influences often exerted a profound influence on the firing of the neurons, and their spatiotemporal organization was predictive of trial-to-trial variations in the latency of saccades. This suggests that the suppressive inputs to SC neurons can exhibit a profound influence on saccades, even when the stimuli that activate them are not perceptually salient.

By analyzing RFs at various time points relative to the saccade, we also obtained a characterization of the influence of oculomotor activity on visual coding in the SC. The results were qualitatively quite similar to the results of studies on saccadic suppression (Burr et al. 1994; Knoll et al. 2011), in which visual sensitivity decreases sharply around the time of saccade onset. Moreover, many neurons in the SC exhibited increased visual sensitivity following a saccade; this pattern of neuronal responses may be related to the postsaccadic enhancement that is observed perceptually (Burr et al. 1994) and in the cortex (Ibbotson et al. 2007, 2008; Kagan et al. 2008; for review Ibbotson and Krekelberg 2011). These results, therefore, confirm the SC as a possible source of corollary discharge signals involved in a number of well-known perceptual effects.

MATERIALS AND METHODS

Physiological Procedures

Two adult male rhesus monkeys took part in the experiments. Each monkey underwent a sterile surgical procedure to implant a headpost and recording cylinder over the SC, as described in detail elsewhere (Choi and Guitton 2006). Eye position was recorded by a video eye-tracker (EyeLink 1000, SR Research) for one monkey and by an implanted scleral eye coil (Robinson 1963) for the other monkey; the sampling rate for both systems was 1,000 Hz. After a postoperative recovery period, the monkeys were seated in a primate chair (Crist Instruments) with their heads fixed and trained to maintain fixation and to make visually guided and delayed saccades toward stimuli presented on a screen. All procedures were approved by the Animal Care Committee of the Montreal Neurological Institute and were in compliance with regulations established by the Canadian Council of Animal Care.

The SC was identified based on an anatomical MRI scan, as well as the physiological pattern of visual and saccade-related neuronal responses. Recordings were performed using tungsten microelectrodes (FHC) with a typical impedance of ~ 2 M Ω . The signal was sampled at 40 kHz. Single units were identified online and later resorted offline using spike sorting software (Plexon).

Behavioral Paradigms

Visual stimuli were generated using a Pentium III PC computer at a spatial resolution of 800×600 pixels and a presentation frame rate of 85 Hz. The frames were programmed in Matlab version 7.0 using the Psychophysics Toolbox (Brainard 1997; Pelli 1997) and back-projected onto a semitransparent screen by a CRT video projector (Electrohome 8000). The screen covered an area of $80 \times 50^\circ$ of visual angle at a viewing distance of 78 cm. The monkeys were required to direct gaze to within $\pm 2.5^\circ$ around the fixation point or saccade target to obtain a small amount of water or juice at the end of each trial.

Sparse noise-mapping task. As described in detail in a previous paper (Churan et al. 2011), we used a sparse noise stimulus to map RFs during saccadic eye movements. In this paradigm, rapid sequences of visual stimuli are presented, such that all relevant spatial and temporal positions can be explored during the course of a single experiment. Our adaptation of the stimulus included a saccade target

that changed position periodically, so that RFs could be mapped at different time periods relative to each saccade.

The sparse noise stimulus consisted of 50% black (<0.001 cd/m 2) and 50% white (30.5 cd/m 2) squares presented at random positions on a gray background (7.0 cd/m 2) (Fig. 1A). The positions of the black and white squares changed randomly at the frame rate of 85 Hz. The size of the squares and the percentage of the screen covered by the stimuli were adjusted individually for each neuron to obtain strong visual responses. Across recordings the size of the squares varied between 1° and 5° (side length), and they covered between 2% and 5% of the screen area; typical values were a size of 3° , covering 4% of the screen. The monkey made visually guided saccades to small ($\sim 10'$ arc) red targets that appeared on the flickering background. In some sessions, the saccade target positions were arranged as a square (Fig. 1A), with the next target appearing either at the adjacent horizontal or the adjacent vertical position relative to the current fixation (for an animated example of the stimulus, see supplemental video in Churan et al. 2011). In this way, the direction of the next saccade was not entirely predictable before the saccade target appeared. The remaining sessions involved only two target locations that were placed so as to elicit only horizontal saccades. In this case, the direction (left or right) and amplitude of the next saccade were fully predictable. Although previous work would suggest that the spatial predictability of the saccade target location should affect the preparatory motor activity in some classes of SC neurons (Basso and Wurtz 1997; Dorris and Munoz 1998), the general pattern of neuronal responses in our data was consistent across these two conditions, and so we have combined the data for the analysis presented here. Although it may have been informative to vary the predictability of the saccade target locations more systematically, we typically required many repetitions of each saccade to obtain reliable estimates of perisaccadic RFs. Thus the behavioral tasks were limited to these two conditions.

The amplitude of the saccades in each recording was constant, but it varied between 10° and 20° across recordings. At the beginning of each trial, there was a random 400- to 1,200-ms fixation period required before the saccade target was presented and the fixation point disappeared. The monkey was allowed to make a visually guided saccade to the target immediately after its appearance and was required to hold fixation on the target for 200 ms to obtain the reward. Typically 2,000–3,000 trials were collected during each recording session.

Delayed saccade task. To determine the visual and motor responses of each neuron, we trained the monkeys to perform a delayed saccade task. In this task, the monkey had to fixate a spot at the center of the screen, while a saccade target was presented at one of 32 randomly interleaved positions (4 amplitudes: 5° , 10° , 15° , and 20° ; 8 directions, covering the contralateral as well as the ipsilateral visual hemifield). Following the appearance of the saccade target, the monkey had to maintain fixation for another 300–700 ms until the fixation point disappeared, after which the saccade was executed. After the saccade, the monkey had to keep fixating on the saccade target for another 300–500 ms to receive a reward.

Data Analysis

The procedures used for analysis of eye movements, as well as for the calculation of RFs, were written in MATLAB (The MathWorks).

Calculation of the RFs. For all of the analyses described below, we first converted the positions of the visual stimuli into retinal coordinates by subtracting the eye position recorded at the time of stimulus presentation from the position of the stimulus in screen coordinates. Space-time RFs were then calculated as the spike-triggered averages (STAs) of sparse noise stimuli in retinal coordinates.

The STA is defined as the average of all stimuli that preceded a spike at a given latency τ . A conventional analysis would involve computing the STA using all available spikes, but in this work we

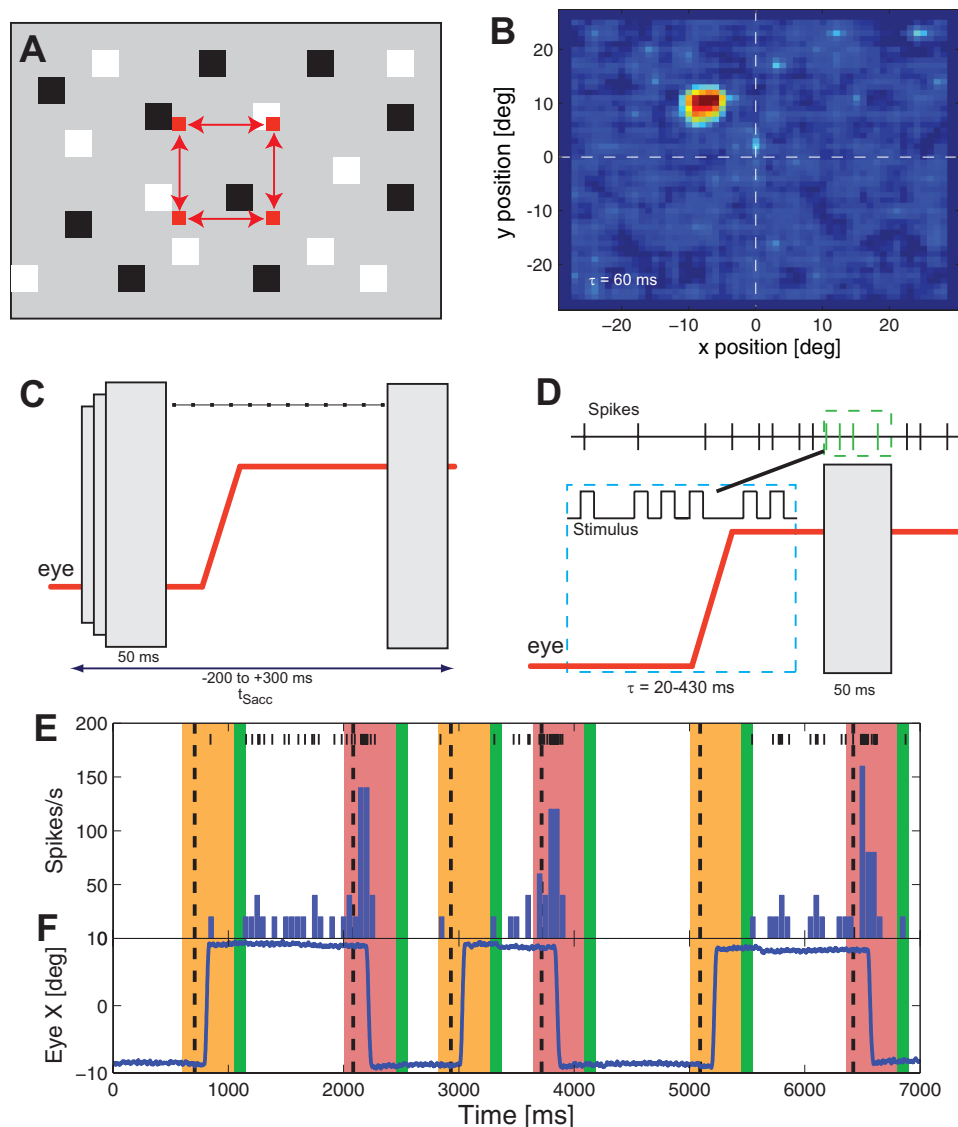


Fig. 1. Description of the method of perisaccadic reverse correlation. *A*: spatial layout of the sparse noise-mapping task. The monkey made saccades (red arrows) to visual targets (red squares) presented on a flickering background, which consisted of a sparse pattern of black and white rectangles changing position randomly at 85 Hz. In some configurations, only two alternate saccade targets were presented, triggering horizontal leftward and rightward saccades (not shown in this figure). *B*: example result of the analysis, showing the receptive fields (RFs) position in retinal coordinates. Yellow and red colors represent a high spike-triggered average (STA), indicating a strong correlation between stimuli at the respective positions and the spiking activity. *C*: for some analyses, perisaccadic RFs were calculated in time windows of 50-ms duration that were shifted in steps of 10 ms between 200 ms before and 300 ms after saccade onset. t_{sacc} , Saccade time. *D*: spikes found in each 50-ms time window were correlated with stimuli that occurred between 20 ms and 430 ms earlier. *E* and *F*: example of the perisaccadic spiking activity (*E*) from a buildup neuron and the simultaneously recorded eye movements (*F*), illustrating the time windows used in the calculation of perisaccadic RFs. The perisaccadic RFs were analyzed in time windows between 200 ms before and 350 ms after the onset of the saccades. These are shown for ipsiversive saccades as orange bars and for contraversive saccades as red bars. The last 100 ms in each perisaccadic time period were used as baseline (green bars). The vertical dashed line shows the time of presentation of the saccade target.

were interested in determining how the RFs changed around the time of a saccade. We, therefore, computed separate STAs using spikes that occurred at specific time points relative to each saccade. For a perisaccadic time T , the STA was computed as:

$$\text{STA}(x, y, \tau, T) = \frac{\sum_{i=1}^{n(T)} s(x, y, t_i - \tau)}{n(T)} \quad (1)$$

Here s is the sparse noise stimulus, and $n(T)$ represents the total number of spikes recorded across all trials at the perisaccadic time T . We defined a fixation STA as the STA computed using a range of values of T that fell between the time 250 ms after the start of fixation and the onset of the next saccade target. Other time windows could be defined analogously relative to saccade onset (gray rectangles in Fig. 1C); specific examples of these time windows are shown as colored regions in Fig. 1, *E* and *F*, and described in detail below.

Because the responses to black and white stimuli were generally very similar (see also Harutiunian-Kozak et al. 1973), we treated them identically for the purposes of the analysis. Thus the value of s at any point in time was either 0 (for no stimulus) or 1 (for a black or white stimulus). The retinal position (x and y) was sampled at a resolution of 1° , and the latency τ was sampled in steps of 5 ms within the range 20–430 ms.

The STA represents the average stimulus preceding each spike by a certain delay. Thus a positive STA indicates that a black or white stimulus element at a particular point tended to elicit a spike at the appropriate latency. However, because the equivalence of the black and white stimuli caused the average stimulus value to be nonzero, the STA would be nonzero even if the spike times were random with respect to the stimulus. To remove this bias, we normalized the STA (STA_n) by subtracting the mean stimulus \bar{s} :

$$\begin{aligned} \text{STA}_n(x, y, \tau, T) &= \frac{\sum_{i=1}^{n(T)} [s(x, y, t_i - \tau) - \bar{s}]}{n(T)} \\ &= \text{STA}(x, y, \tau, T) - \bar{s} \end{aligned} \quad (2)$$

Thus an STA_n at a certain position in space and time (x, y, τ, T) with a value of 0 represents a response that would be expected to result from spiking activity that is unrelated to the visual stimulus, while $\text{STA}_n > 0$ indicates an activation of the neuron by the stimulus, and $\text{STA}_n < 0$ indicates suppression by the stimulus. In the following, the integral of the STA_n in a defined spatiotemporal window will be referred to as the STA strength.

Fixation RF. The fixation RF was estimated using Eq. 2 based on a time window that started at $T = 250$ ms after the end of each saccade

and ended at the onset of the next saccade target. Within this time window, we estimated each neuron's RF by finding the regions of visual space in which visual stimuli elicited significant responses during fixation. For this, we first calculated for each neuron the STA_n based on Eq. 2. Next we calculated a zero-correlation STA_n (STA_{n0}) using the spike trains of the same neuron and randomly shuffling the order of the visual inputs. This procedure was repeated 100 times, yielding a distribution of STA_{n0} . We considered a pixel to be significantly activated if its STA_n value exceeded the mean ± 2 SDs of the distribution of values for STA_{n0} . As this statistical criterion is based on individual pixels, it is by itself insufficient to define the RF, since many single pixels outside the RF would be expected to be significantly activated by chance. To differentiate between the RF and spurious activation outside the RF, we used the size of clusters of adjacent significant space-time data points as a second criterion. We calculated the sizes of these clusters in the STA_n and compared them to the cluster sizes obtained from the 100 random baseline samples of the STA_{n0} . Clusters in the real data with a size larger than 95% of the largest cluster sizes found in the STA_{n0} distribution were considered to be RFs. Because previous publications have reported the shape of SC RFs to be approximately circular or elliptical (Cyander and Berman 1972, Marocco and Li 1977), we fitted the excitatory and suppressive components of each RF to a two-dimensional Gaussian. As part of this procedure, we first integrated the excitatory and the suppressive responses separately over time and then fitted a two-dimensional Gaussian to each using a least squares method. To ensure that this approach did not bias our conclusions, we also calculated a nonparametric estimate (the center of gravity) of the centers of excitatory and suppressive RF components for comparison with the results of the Gaussian fits. The center of gravity represents the average position of each RF component weighted by the strength of the component at different spatial positions.

Perisaccadic RF. We also aimed to estimate RFs in various time periods relative to each saccade. Because these time periods were necessarily quite short (50–100 ms, Fig. 1, C and D) and the number of spikes accumulated in these time windows over the duration of the experiment was often low (typically ~ 100 – 200 when no motor activity was present), a full space-time characterization of excitatory and suppressive RF components was not possible. We, therefore, focused on the excitatory RF components and integrated the temporal response where possible, as described in RESULTS.

Estimates of the spatial positions of the perisaccadic RF centers were based on the STA_n for spikes recorded in 100-ms time windows corresponding to four different perisaccadic times: early presaccadic ($T = 200$ – 100 ms before the saccade onset), perisaccadic ($T = 60$ ms before to 40 ms after), early postsaccadic ($T = 140$ – 240 ms after), and a baseline period (250–350 ms after each saccade). These RFs were fit with two-dimensional Gaussians, and the centers of the fitted Gaussians were used as estimates of the RF position.

To compare the perisaccadic changes in spiking activity with changes in the STA strength, we analyzed the data in time windows of 50-ms duration that were shifted in 10-ms steps between 200 ms before and 300 ms after the onset of the saccade (orange and red bars in Fig. 1, E and F). In each time window, we measured the number of spikes and the average STA_n in a region that was defined based on the excitatory part of the fixation RF. The baseline activity and STA_n were defined in a time window between 300 ms and 400 ms after the saccade onset (green bars in Fig. 1, E and F).

Although we were interested in estimating the influence of saccades on visual RFs, the retinal disturbances caused by each saccade precluded analysis of some perisaccadic data. In particular, the retinal positions of stimuli presented during the saccade could not be estimated accurately due to the high velocity of the eye movements. Thus estimates of the STA were unreliable for stimuli presented during the saccade and for spikes immediately following the saccade. Because we typically binned spikes into 50-ms time windows, we also considered bins that began immediately before saccade onset to be

potentially unreliable, as these bins could contain spikes due to stimuli presented near saccade onset. By these conservative criteria, bins beginning between 10 ms before a saccade and 110 ms after a saccade were excluded from detailed statistical analysis. For completeness, we have nevertheless computed the STAs in these bins and demarcated them with vertical lines in Figs. 7–9.

Predicting the effects of motor activity on visual RFs. Spiking activity in the intermediate layers of SC changes substantially around the time of saccades. In particular, saccades directed into the movement field of a neuron yield strong increases in spiking activity due to the preparatory and motor responses of the neurons. Because this motor activity is by definition unrelated to the visual stimulus, it is expected to decrease the strength of the perisaccadic STA_n . This is based on the fact that the STA_n for nonvisual spikes is zero, as described in Eq. 2. Consequently, the numerator of Eq. 2 is insensitive to motor activity, while the denominator will increase during a motor burst, leading to a decreased STA_n . In other words, the motor burst leads to a decorrelation of the spike train from the visual stimulus.

To separate this effect from any potential changes in the strength of visual inputs, we calculated the extent to which the STA_n would be expected to change if the neurons combined motor and visual activity in a purely additive fashion. For a perisaccadic time T , the expected change in the strength of the STA_n is simply a scaling of the STA_n in proportion to the increase in the spike rate above the baseline rate, as follows:

$$STA_{n,pred}(x, y, \tau, T) = \frac{\sum_{i=1}^{n(T)} [s(x, y, t_i - \tau) - \bar{s}]}{n(T)} \quad (3)$$

$$= STA_{n,Base}(x, y, \tau) * \frac{n_{Base}}{n(T)}$$

where $STA_{n,pred}$ is the predicted STA_n at the perisaccadic time T , $STA_{n,Base}$ is the base STA_n obtained during fixation, n_{Base} is the average base spiking activity during fixation, and $n(T)$ is the spiking activity in the time window at perisaccadic time T . This predicts that the STA will decrease in proportion to the increase in spike rate $n(T)$ above the baseline n_{Base} . Although we often observed cases in which the spike rate decreased around the time of a saccade, we did not attempt to analyze them in this way because we often found that $n(T)$ approached zero during these periods. Thus Eq. 3 was only applied when $n(T) \geq n_{Base}$. Because this formulation assumes that the contribution of visual responses remains constant during the saccade, any differences between the observed data and the output of Eq. 3 can be interpreted as perisaccadic changes in the strength of the visual inputs.

Influence of sparse noise stimulus on the timing of saccades. Although the sparse noise stimulus is random in space and time, the distribution of stimulus elements can be biased on any one trial. These statistical fluctuations are in fact the basis of the STA described above. Because the sparse noise stimuli were distractors in the context of the saccade task, we decided to investigate the effect of fluctuations in the sparse noise stimuli on the saccadic reaction times (SRTs). To this end, we calculated saccade-triggered stimulus averages, which are the average stimuli that were presented at a certain time (τ) before the onset of a saccade. These provided spatiotemporal distributions of the effects of distractors on SRTs.

The values of τ used in this calculation were in the range of -300 ms to 0 ms in steps of 10 ms. As with STAs, a saccade-triggered average at a certain retinal position and a certain presaccadic time τ provides a measure of the influence of that stimulus on a saccade that starts τ ms later. For instance, if there were a relatively low concentration of stimuli at position (x, y) and delay τ , this would imply that a stimulus at that position can inhibit the initiation of a saccade τ ms later. We examined the effects of distractors at positions within an area of $\pm 30^\circ$ horizontal and $\pm 20^\circ$ vertical around the fixation point.

Classification of Neurons

After excluding neurons that lacked visual responses, the sample consisted of 168 neurons (96 from *monkey 1*, 72 from *monkey 2*). These neurons were further categorized based on their perisaccadic motor responses as being either purely visual, visuomotor, or buildup neurons, with the latter showing preparatory activity in the delayed saccade paradigm and/or in the sparse noise paradigm. A breakdown of the cell types is provided in Table 1.

Although we have not attempted to reconstruct our electrode tracks, it is likely that most of our recordings came from the intermediate layers of the SC. Most of the neurons showed motor responses (Table 1), and the few purely visual cells included in the analysis were generally found at roughly the same depth as these visuomotor neurons, despite the fact that most purely visual neurons are located in the superficial layers (Goldberg and Wurtz 1972). It is possible that some or all of these visual neurons were “quasivisual” cells (Mays and Sparks 1980), which can only be identified with certainty in a double-saccade task.

RESULTS

In this work we probed visual RFs in the macaque SC with a mapping stimulus composed of black and white spots displayed at random positions on a gray background (Fig. 1). Previous work has shown that this stimulus, in combination with standard reverse correlation analysis, permits recovery of the detailed spatial and temporal structure of visual RFs (Jones and Palmer, 1987; Pack et al. 2006). A novel aspect of the approach used here is that we required monkeys to make saccades during the presentation of the mapping stimulus. Thus we were able to characterize RFs in SC during fixation and to determine how they changed around the time of a saccade. We estimated RFs at various time points relative to saccade onset in three classes of neurons (visuomotor, build-up, and purely visual) that have often been studied in previous work in the SC.

Structure of Receptive Fields During Fixation

In the first part of the study, we investigated the spatial and temporal properties of the excitatory centers and suppressive surrounds of SC RFs in time periods of steady fixation between saccades.

Spatial organization of SC RFs. Figure 2 shows examples of the types of RFs we encountered in the SC, with each column corresponding to a different neuron. Red colors indicate a strong correlation between spikes and visual stimuli at the corresponding point in space and time. Blue colors indicate a negative correlation, which is associated with suppression. The first row shows the two-dimensional spatial structure of the RFs in retinal coordinates at the peak correlation delay. The second row shows a horizontal cross section through the same RFs at different latencies between the stimulus and the spiking response. The third row shows the spatial structure of the RF as an integral of the temporal impulse response function at each spatial position.

The RF of the neuron in the first column is purely excitatory at all points in space and time. In contrast, the other RFs have both excitatory and suppressive components. For the neuron in the middle column, the suppressive component is coincident spatially, but delayed temporally relative to the excitatory component. The RF in the third column exhibits excitatory and suppressive components at different times and at different spatial positions.

In our sample of 168 neurons, 96 (57%) showed purely excitatory RFs (see MATERIALS AND METHODS for statistical criteria), while the rest exhibited excitatory and suppressive interactions of varying degrees of complexity. As shown in Table 1, the structure of the visual RFs was independent of neuronal classification, since the presence of suppressive components was equally distributed over all types of neurons ($P > 0.05$, χ^2 test). However, as also shown in Table 1, there were significantly more neurons with inhibitory surrounds found in *monkey W* than *monkey L* ($P < 0.05$, χ^2 test).

To quantify the spatial RF structure for the population of SC neurons, we fit each excitatory and suppressive component with a two-dimensional Gaussian function, as described in MATERIALS AND METHODS. These functions typically provided a very good fit to the RF structure, with the median r^2 values being 0.95 for the excitatory components and 0.85 for the suppressive components. This analysis provided estimates of the sizes and positions of both the excitatory and suppressive components of each neuron's RF.

Figure 3, *B–E*, shows the excitatory and suppressive spatial components for four example neurons. In some cases, the two components differ in size or spatial position, and these differences are plotted in Fig. 3*A* for the population of SC neurons. Here the normalized differences in the size of the excitatory and the suppressive components are plotted against the normalized differences in their positions (i.e., the distance between their centers). The marginal distribution along the x-axis is centered near zero (mean = -0.014), indicating that, although there were sometimes large differences in the sizes of the two RF components for individual neurons, there was no general trend for the whole population. The differences in position are plotted on the y-axis for Fig. 3*A* as the absolute distance of the centers of the excitatory and the suppressive components normalized by the RF radius. For many neurons, the separation between the two components was a sizeable portion of the RF radius: For 49% (34/72) of the neurons, the centers were separated by more than 20% of the RF radius, and for 24% (17/72) they were separated by more than 50% of the RF radius. Notably for these neurons, the suppressive component was often shifted toward the fovea, as is clear in the two example neurons shown in Fig. 3, *B* and *C*.

To determine whether the foveal bias for suppression was seen in the SC population, we estimated the relative positions of excitatory and suppressive components using the method

Table 1. Frequency of significant excitatory and suppressive responses in each of the three neuronal categories

	Visuomotor	Buildup	Visual	Sum
Excitatory only	49 (27/22)	31 (10/21)	16 (0/16)	96 (37/59)
Excitatory and suppressive	28 (25/3)	35 (32/3)	9 (2/7)	72 (59/13)
Sum	77 (52/25)	66 (42/24)	25 (2/23)	168 (96/72)

Separate counts for the two monkeys (W/L) are shown in parentheses.

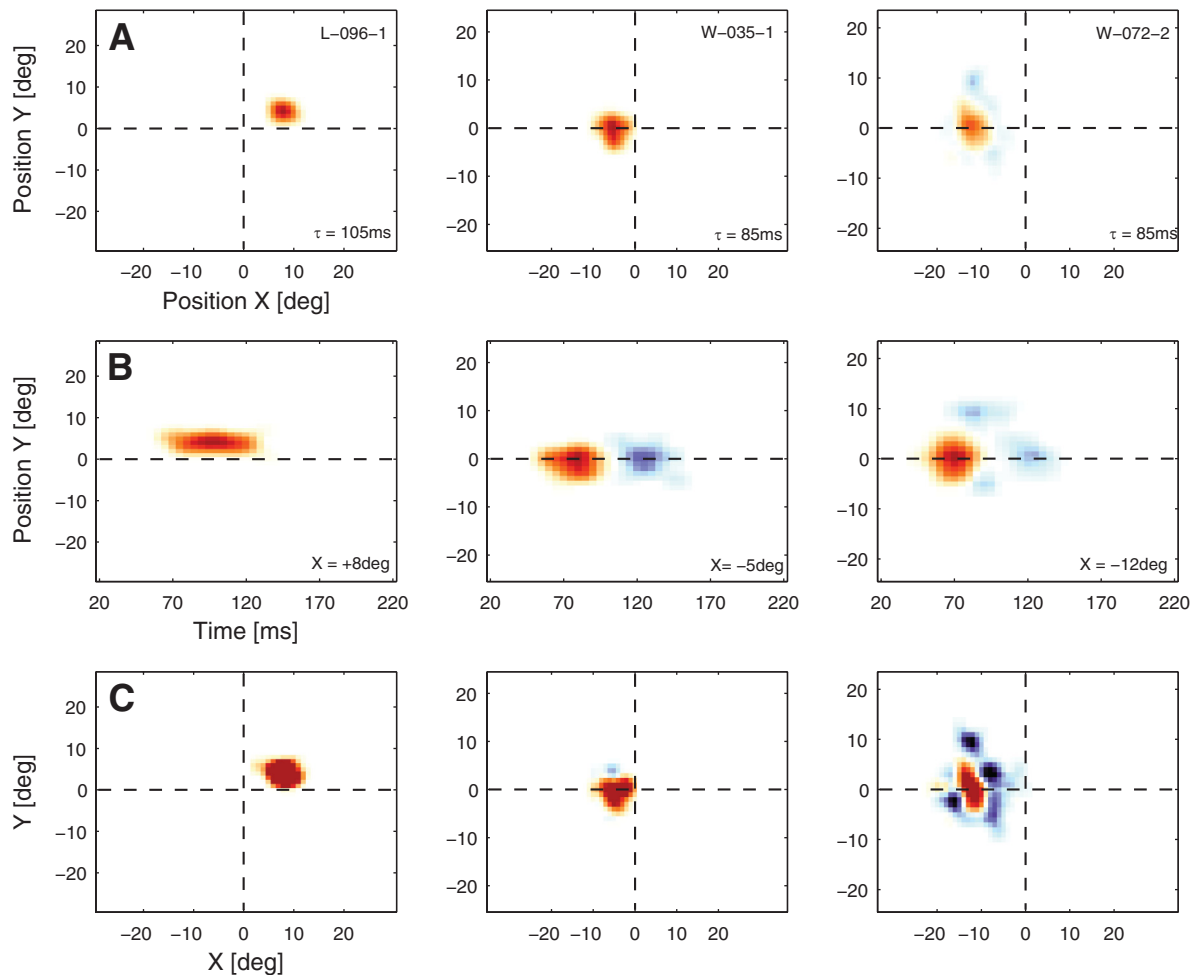


Fig. 2. Three-dimensional RF structures of 3 example superior colliculus (SC) neurons during fixation. Red colors indicate excitatory RF areas [positive normalized STA (STA_n)], while blue colors mark suppressive areas (negative STA_n). A: spatial position of the RFs in retinal coordinates at a time τ that shows the strongest excitatory responses. B: space-time plot showing the succession of excitatory and inhibitory phases over time. C: spatial structure of each neuron's STA_n integrated across time.

illustrated in Fig. 4A. This involved calculating the angle between a line drawn from the fovea to the excitatory RF and a line drawn between the centers of the excitatory and suppressive RF components. Thus an angle of 0 indicates a suppressive field oriented toward the fovea, and an angle of 180 indicates a suppressive field oriented toward the periphery. Across the population, there is a strong bias toward suppressive components that are located on the foveal side of the excitatory component ($P < 0.05$, blue distribution in Fig. 4B). This finding was not due to any bias in the Gaussian fits, as a nonparametric estimate based on the center of gravity of each component yielded nearly identical estimates of positions of the excitatory and inhibitory centers (median position difference was 0.53° for excitatory components and 0.67° for suppressive components).

In principle, this bias could result from the limited size of our spatial display: Peripheral surrounds might have extended beyond the borders of our projection screen. Alternatively the bias could have resulted from random sampling of RFs with very small offsets between the excitatory and suppressive components. To examine these possibilities, we investigated the orientation of the surrounds for a subsample of 45 neurons in which the eccentricity of the center of the excitatory com-

ponent was smaller than 20° and the two components were at least 0.1 RF radii apart. For this subpopulation (Fig. 4B, red) the foveal bias was still significant ($P < 0.05$, Kolmogorov-Smirnov test), indicating that the observed asymmetry of RF surrounds was unlikely to be a sampling artifact.

The temporal properties of excitatory and suppressive responses. In addition to being shifted in space relative to the excitatory RFs, the suppressive components were generally delayed in time, as demonstrated in the examples shown in Fig. 2B. Figure 5 shows the range of temporal responses observed for the excitatory and suppressive components of the response across the three different categories of collicular neurons. In this analysis, we also divided suppressive influences into those that were spatially coincident with the excitatory RFs (as in the second column of Fig. 2B) and those that were not (as in the third column of Fig. 2B). We refer to these two categories as aligned and misaligned suppression. The latency of both types of suppressive responses was significantly ($P < 0.001$, *t*-test for each) longer than that for the excitatory responses. In addition, the latency of the aligned suppression was significantly longer ($P = 0.001$, *t*-test) than the latency of the misaligned suppression. The foveal bias of the spatial surrounds reported in the previous section was present for sur-

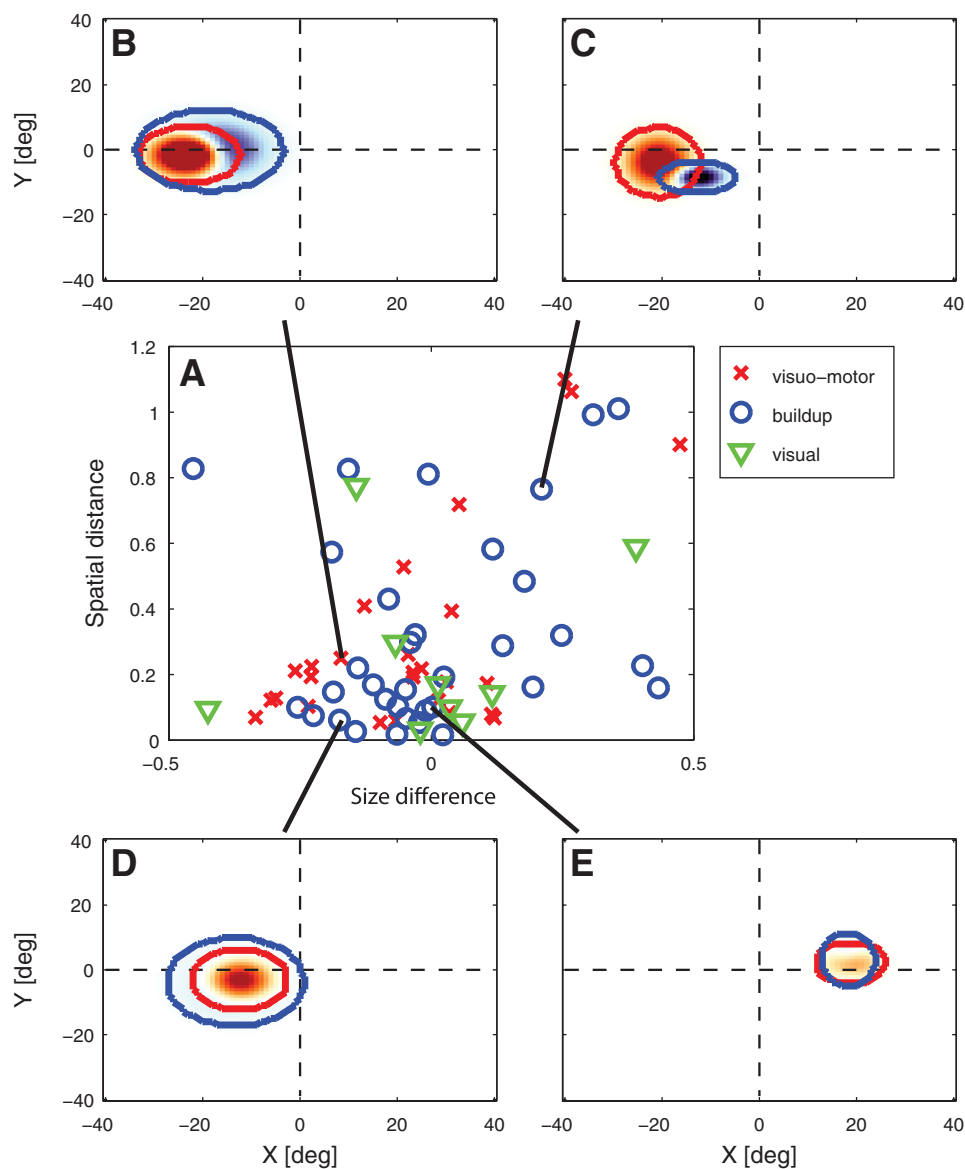


Fig. 3. A: relationship between excitatory and the suppressive RF components described by the normalized difference of their sizes and the spatial distance of their centers. The different categories of neurons are represented as different symbols, with red crosses corresponding to visuomotor neurons, blue circles to buildup neurons, and green triangles to visual neurons. Negative values for the normalized size difference indicate that the suppressive component was larger than the excitatory component, while positive values indicate a larger excitatory component. B–E: RFs of example neurons demonstrating different spatial configurations of excitatory and suppressive RF components. Red and blue lines mark the borders of the excitatory and suppressive components defined at 2 SDs of the two-dimensional Gaussian fits.

rounds that appeared simultaneously with the excitatory centers ($P < 0.01$, Kolmogorov-Smirnov test) and for those that appeared after the excitatory centers ($P = 0.06$, Kolmogorov-Smirnov test). Thus our results indicate that suppressive visual influences on SC neurons are shifted in space and time relative to their excitatory counterparts, and that the foveal bias is present throughout the duration of the suppressive response. In the next section, we examined potential behavioral correlates of this RF organization.

Effects of Visual Receptive Fields on Saccades

The preceding section demonstrates a bias in SC RF organization, such that suppression is typically concentrated to the foveal side of excitation. Although strong surrounds were only found in a minority of neurons, the foveal bias was quite consistent within this population. To determine whether this bias exerted an influence on eye movements, we analyzed the influence of the sparse noise stimulus on the characteristics of the saccades made by the animals during the mapping procedure. This approach allowed us to test the hypothesis that the

spatial and temporal properties of the surround affected the animals' oculomotor behavior. If the surround affected behavior, we would expect to find that trials in which elements of the mapping stimulus appeared at the foveal side of the saccade target would be associated with delayed saccades.

To test this possibility we computed saccade-triggered averages of the stimulus. These are the average spatial distributions of stimuli that preceded the saccades by a certain time. As described in MATERIALS AND METHODS, they provide a measure of the influence of stimuli at different spatial locations and pre-saccadic times on the SRTs.

Figure 6A shows the results for one monkey (*monkey W*), based on 42 sessions, each with an average of 1,022 horizontal saccades (amplitude 20°) in each of two movement directions (leftward and rightward). The second monkey (L) generally exhibited weaker surround suppression in SC recordings (Table 1) and on the behavioral measures described in this section. Here, orange colors correspond to a high probability of a stimulus at a particular point in space and time, while green colors indicate low stimulus probabilities. The second and third

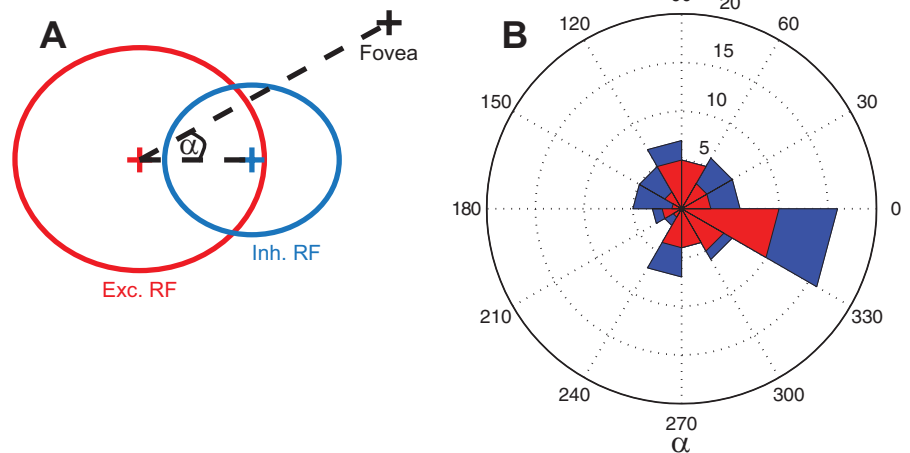


Fig. 4. *A*: the calculation of the angle α between the center of the excitatory and the center of the suppressive part of the RF with respect to the fovea. *B*: distribution of the angle α for the whole sample (blue) and for the subsample of 45 neurons with a relatively large separation between the excitatory and suppressive components and a small eccentricity (red).

rows of Fig. 6*A* show that stimuli on the foveal side of the saccade target (black X) are more likely to occur ~ 110 ms before saccade onset but less likely at ~ 80 ms before saccade onset. Note that the different colors in Fig. 6 do not correspond to excitation or suppression, as in previous figures, but rather to the presence or absence of stimuli at different times relative to saccade onset. These results can be interpreted based on the suppressive influences reported in the previous sections: stimuli flashed on the foveal side of the saccade target fall into the suppressive area of the neurons that encode the saccade vector. As a result, they delay the execution of saccades that would normally occur roughly 80 ms later, increasing the latency by roughly 30 ms. This interpretation is consistent with an effect of surrounds on motor activity, given the latencies for surround suppression shown in Fig. 5.

Figure 6*B* shows the strength of the surround effect across a range of spatial positions and temporal delays. Here we have combined the data from leftward and rightward movements and sampled time more finely. The results indicate that the effect of stimulus position is restricted to a brief time window between 70 ms and 110 ms before saccade onset and to a small area of $\sim 10^\circ$ on the foveal side of the saccade target. Figure 6*C*

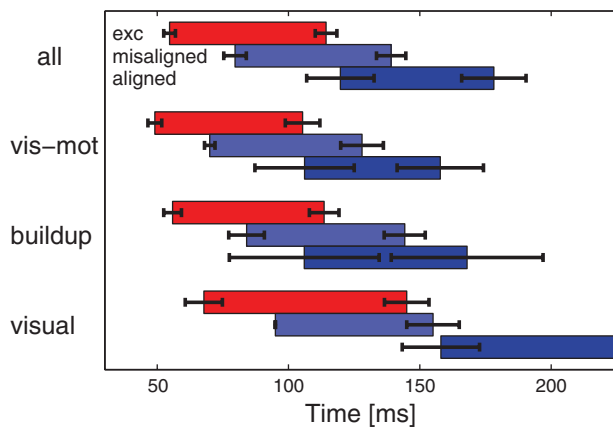


Fig. 5. Mean and SE of the beginnings and ends of excitatory (red bars) and suppressive responses. The suppressive responses of neurons are split into two categories: those without (misaligned, light blue) and those with (aligned, dark blue) preceding excitatory responses at the same spatial location. The results are shown separately for the whole sample and for the three categories of neurons.

summarizes the temporal structure of the effect by spatially integrating the data in Fig. 6*B*.

Effects of Saccades on Visual Receptive Fields

Psychophysical studies have revealed a number of profound changes in visual sensitivity that occur around the time of a saccade (Bridgeman et al. 1975; Diamond et al. 2000; Holt 1903). Generally, visual sensitivity begins to decrease roughly 100 ms before a saccade, remains low during the saccade, and often increases immediately after a saccade (postsaccadic enhancement; Burr et al. 1994; Ibbotson et al. 2007, 2008; Kagan et al. 2008). To provide a qualitative comparison of these effects with SC activity, we calculated perisaccadic STAs for 100 SC neurons that fit the inclusion criteria described in MATERIALS AND METHODS.

Figure 7 (*bottom* panels) shows a cross section through the RF of one example neuron (the same as was shown in Fig. 2, *right* column) at different times relative to saccade onset. The responses for contraversive and ipsiversive saccades are shown separately. Here, as in subsequent figures, the firing rate and the STA strength are normalized relative to the baseline obtained during periods of steady fixation. The STA strength is the integral of the STA across a region of interest defined by the spatiotemporal excitatory RF during fixation, which, as shown below, remains roughly constant in retinal coordinates around the time of the saccade. Estimating the overall magnitude of the STA in this way increased the signal-to-noise ratio substantially, so that we could detect changes in visual sensitivity at various intervals relative to saccade onset. Note that, in this and in subsequent figures, the vertical lines demarcate time periods during which the estimation of the STA was rendered potentially unreliable by the retinal motion associated with the saccade.

For contraversive saccades, the strength of the STA in Fig. 7 changes dramatically around the time of saccade onset ($t = 0$ on the x -axis). The bright orange colors indicate a strong STA that essentially disappears just before the onset of the contraversive saccade and reappears after saccade offset. As shown in the *top* panels of Fig. 7, these perisaccadic changes in the strength of the STA follow the time course of corresponding changes in the firing rates of the neurons.

From Fig. 7 it also appears that the retinal position of the RF varies somewhat at different intervals relative to the saccade.

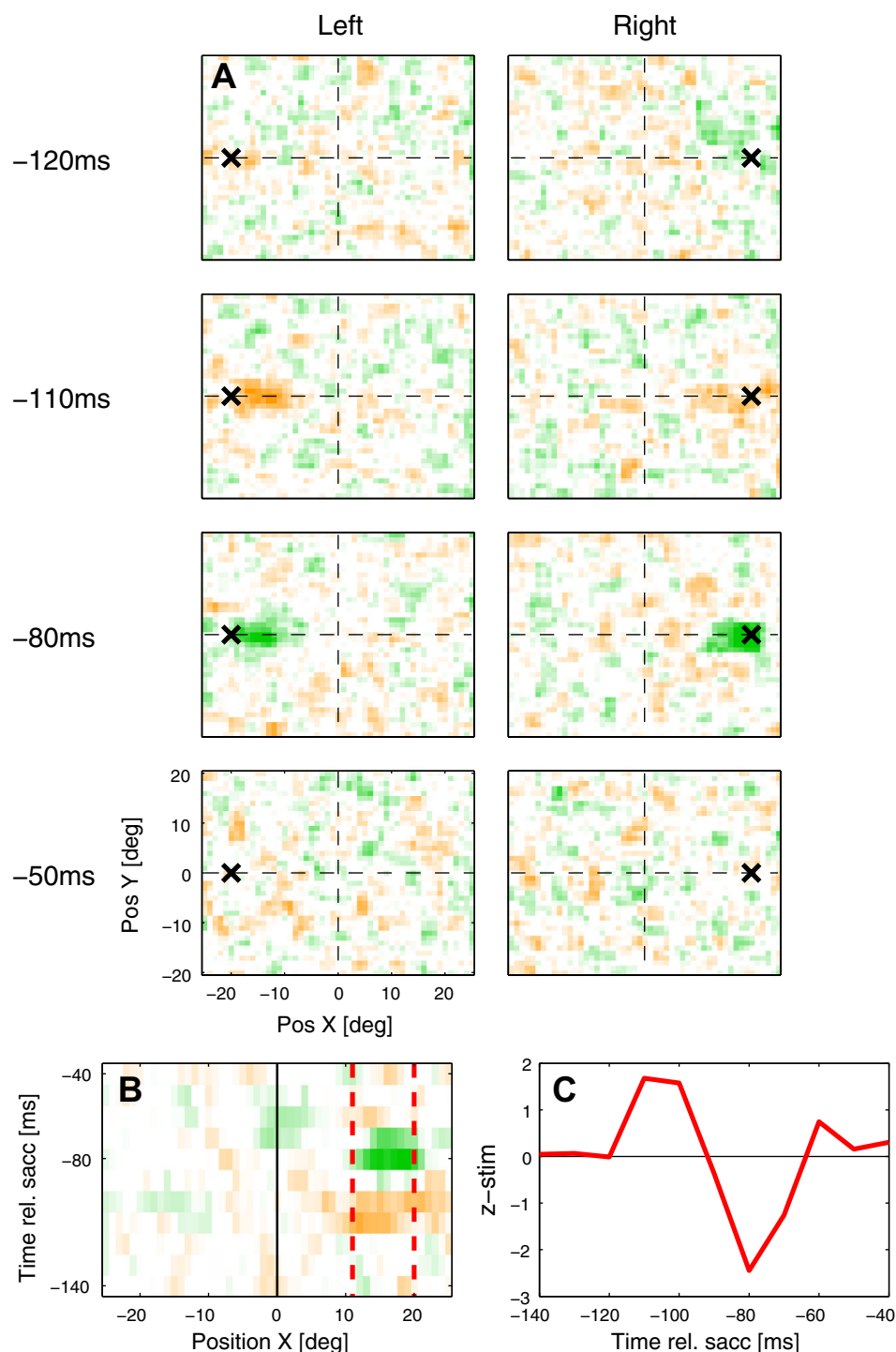


Fig. 6. *A*: STAs of the sparse noise stimuli at different times before the onset of leftward and rightward saccades. The positions are shown in retinal coordinates. The position of the saccade target is marked as a black cross. Green colors indicate that stimuli appeared less often at the respective position and time, while orange colors indicate a high concentration of stimuli. *B*: spatiotemporal profile of the effect of sparse noise stimuli shows the changes of one horizontal line of *A* (at $Y = 0^\circ$) over time. The leftward and rightward saccade directions were collapsed by horizontally mirroring the result for leftward saccades and averaging the results. Vertical red lines indicate the spatial area that was used to calculate the temporal profile depicted in *C*. *C*: temporal profile of the saccade triggered averages between $X = 11^\circ$ and $X = 20^\circ$, and at $Y = 0^\circ$.

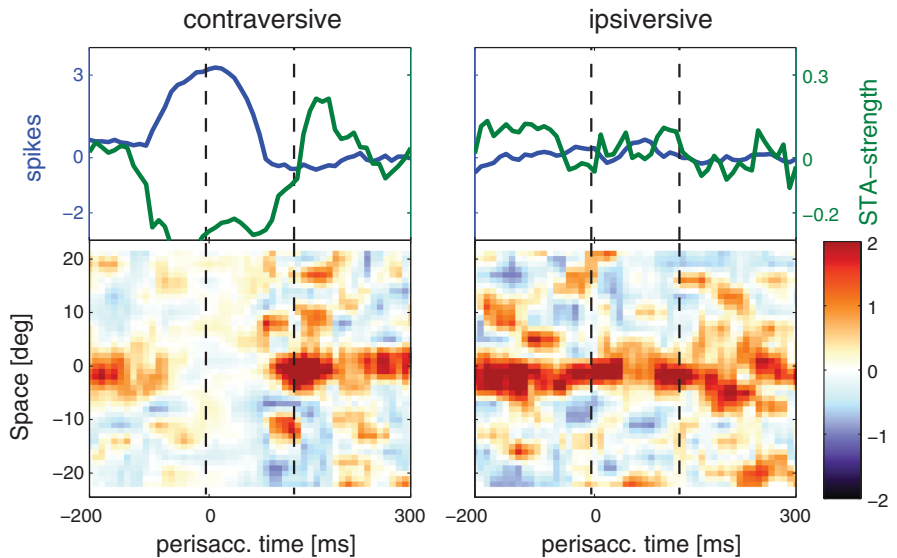
As we have reported previously (Churan et al. 2011), this variation is not related to the RF remapping that has been shown to occur in SC under certain conditions (Dunn et al. 2010; Walker et al. 1995). Indeed, across all pre- and postsaccadic time intervals, the average changes in RF position (see MATERIALS AND METHODS for RF estimation procedure) were always less than 1° of visual angle. These changes exhibited no discernible relationship to the saccade vector. Based on this analysis, we conclude that, in this paradigm, saccades are associated with changes in the strength, but not the position of visual RFs.

Mechanisms of Perisaccadic Changes in Visual Sensitivity

The example neuron in Fig. 7 shows a large fluctuation in the STA strength around the time of contraversive saccades (*left* plot). These changes in STA strength are accompanied by changes in the spiking activity, due to perisaccadic motor bursts. Because these motor bursts are by definition unrelated to the visual stimulus, they are likely to be responsible, at least in part, for the weaker STAs observed around the time of the saccade.

To examine this possibility, we compared the mean STA strengths and the spiking activity around the time of con-

Fig. 7. Perisaccadic RF changes for one example neuron for contraversive (*left*) and ipsiversive (*right*) saccades. The *bottom* panels show cross sections through the spatial STA at the peak temporal delay (85 ms). Each data point reflects the visual responses in a 50-ms time window that starts at the time given on the *x*-axes. Shades of red indicate excitatory responses, while shades of blue indicate suppression. The *top* panels show the spiking activity (blue) normalized relative to the base activity that was recorded 250–350 ms after the saccade onset, as well as the normalized average STA strength (green). The dashed lines mark an area in which the data may be influenced by stimuli presented during the saccade. Since our estimates of retinal position of stimuli presented during the saccade are inaccurate, the STA strength within these borders is likely to be underestimated.



traversive saccades for the three categories of neurons. For those neurons that showed distinct motor responses in preliminary testing (visuomotor and buildup neurons), we focused on cells in which the contraversive saccade was made into the movement field. This left us with a sample of 22 visuomotor neurons, 26 buildup neurons, and 18 visual neurons. The average STA strength and spiking activity in 50-ms perisaccadic windows are shown in Fig. 8, *A* and *B*, for the visuomotor (red line), buildup (blue line), and visual (green line) cells.

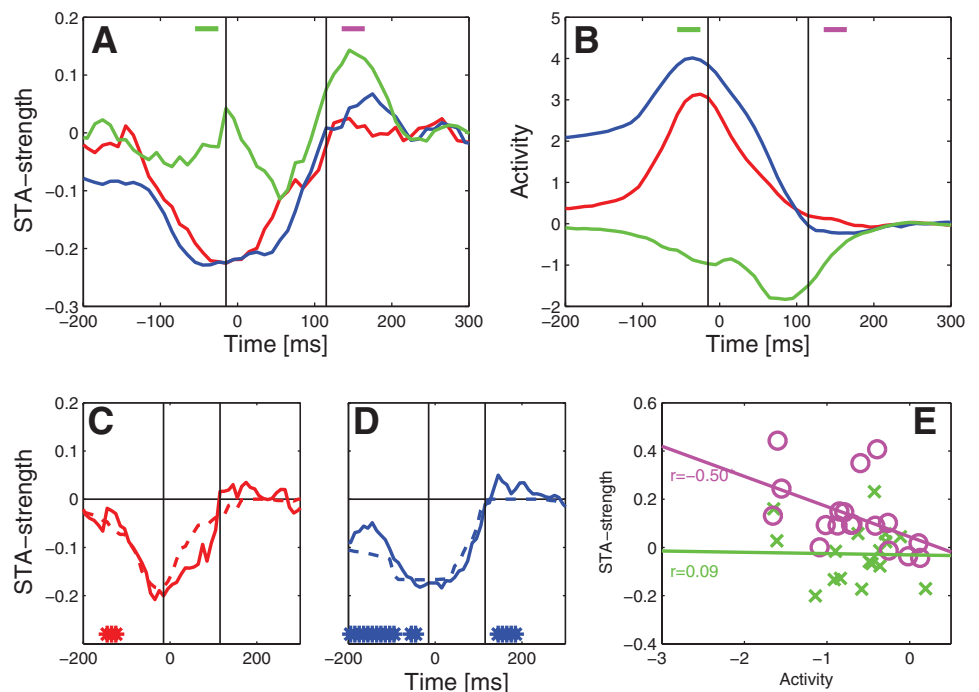
As expected, the spiking activity of visuomotor and buildup neurons increased strongly before the onset of the saccade, and at the same time the STA strength decreased for these two classes of neurons. To test the hypothesis that the increase in motor activity could entirely account for the change in the STA strength, we calculated the change in STA strength that would be expected if all of the observed increases in spike rate were

due to the addition of motor-related spikes (see MATERIALS AND METHODS, Eq. 3). This calculation served as a baseline against which to examine potential perisaccadic changes in the strength of visual inputs.

Figure 8*C* shows that this analysis was quite accurate in predicting the time course of perisaccadic changes for the visuomotor neurons. Statistically, there was a significant difference between the data (solid lines) and the prediction (dashed lines) only during a brief perisaccadic period, as indicated by the asterisks in the figure. This suggests that visuomotor neurons combine visual and motor signals in a roughly linear fashion. In other words, the decrease of the STA seen in these neurons is due almost entirely to the fact that the additional motor activity decorrelates the spike train from the visual stimulus.

For the buildup neurons (Fig. 8*D*), the linear model correctly predicts a decrease of STA strength long before the saccade, but it significantly overestimates the strength of this decrease.

Fig. 8. *A*: normalized STA strength for the three classes of neurons around the time of contraversive saccades. The responses are calculated in 50-ms windows that start at the time indicated on the *x*-axes. Visuomotor neurons are marked as red lines, buildup neurons in blue, and visual neurons in green. Vertical black lines mark the area in which the strength of visual responses is likely to be underestimated, since it is influenced by stimuli presented during the saccade. *B*: normalized spiking activity for the three classes of neurons. *C* and *D*: comparison of the normalized STA strength (solid lines) and the model prediction (dashed lines). Perisaccadic times at which the observed responses differ significantly from the model ($P < 0.05$) are marked with asterisks. *E*: correlation of spiking activity and STA strength for visual neurons in time windows before (green) and after (magenta) the saccade. A significant correlation was found for the postsaccadic but not for the presaccadic period. The time windows used for the calculation are marked in *A* and *B* as green and magenta horizontal bars.



One possible interpretation of this discrepancy is that the preparatory activity in these neurons is due not only to an increase in the strength of motor inputs, but also to an increase in the gain of the visual input. This likely corresponds to the increased contrast sensitivity reported by Li and Basso (2008).

Another difference between the model and the observed visual responses is after the saccade, when all groups of neurons show an increased STA strength. This difference is weak and not significant for visuomotor neurons, but stronger and significant ($P < 0.05$) for the buildup neurons. The postsaccadic increase in STA strength is particularly strong in the visual neurons (Fig. 8A). Note that visual neurons are generally inhibited during this time period (Fig. 8B), so that the model prediction based on increased motor activity was not applicable.

To examine the connection between spiking activity and STA strength in visual neurons in more detail, we plotted presaccadic and postsaccadic firing rates against the STA strengths obtained in the same 50-ms time periods (marked as horizontal lines in Fig. 8, A and B) for all visual neurons in our sample. The results are shown in Fig. 8E. In the presaccadic time period, the spiking activity and STA were uncorrelated (green X's), while after the saccade (purple dots) there was a significant ($P < 0.05$) negative correlation between the two measures. This indicates that those neurons that were strongly inhibited after the saccade showed the strongest postsaccadic enhancement.

The postsaccadic enhancement shown in Fig. 8E could in principle result from visual mechanisms that are stimulated by the retinal motion associated with the saccade. In this case, the enhancement should be insensitive to the saccade direction, as SC neurons are not generally selective for retinal motion direction. To further examine the relationship between firing rate and postsaccadic enhancement, we calculated the average firing rates and STA values for the same neurons during ipsiversive movements (Fig. 9). For ipsiversive saccades, the buildup neurons (blue line), but also to some degree the visual neurons (green line), showed clear pre- and postsaccadic inhibition of their spiking activity (Fig. 9B). However, in contrast to the results for contraversive saccades, the correlations between the spiking activity and the STA strength were not significant for any class of neurons or any time window. Thus neither the presence of inhibition nor the execution of a saccade is sufficient to generate a postsaccadic enhancement of STA strength. Rather the relationship between the inhibition of firing rate and the increase in STA strength is specific to the postsaccadic time window and the execution of contraversive saccades.

In summary, the perisaccadic STA in the SC changes in a manner that is qualitatively similar to perceptual saccadic

suppression and enhancement. The mechanism of suppression appears to be an increase in nonvisual spiking activity, and in buildup cells this is offset somewhat by an increase in visual sensitivity. Postsaccadic enhancement is found in many cells, and it appears to result from a selective mechanism that reduces the impact of nonvisual inputs following contraversive saccades.

DISCUSSION

We investigated the spatiotemporal RF structure of 168 SC neurons in two monkeys in a sparse noise-mapping task. This task allowed us to generate high-resolution estimates of excitatory and suppressive RF components during steady fixation. From these estimates, we were able to predict the effects of particular visual stimuli on the timing and metrics of saccades and to determine how basic RF properties changed around the time of a saccade.

Our mapping procedure allowed us to estimate both excitatory and suppressive contributions to the visual responses of SC neurons. By our statistical criteria, 43% of the neurons showed significant suppressive spatial regions. This is likely to be an underestimate, given that suppressive inputs are often found to be particularly sensitive to the nature of the stimulus, (Barlow et al. 1957; Ichida et al. 2007; Sceniak, et al. 1999; Tsui and Pack 2011), which in our experiments was not optimized for any individual neuron. In the time domain, suppression was generally delayed relative to excitation, so that the sudden onset of a visual stimulus would be expected to generate within the SC a strong transient response that would not be dependent on stimulus size. This is in line with the proposed function of SC as a novelty detector (Boehnke and Munoz 2008; Boehnke et al. 2011; Platt and Withington 1997; Sparks and Nelson 1987) that facilitates orientation toward the appearance of highly salient, novel stimuli. Moreover, the relatively lengthy duration of suppression (150–250 ms after stimulus onset) might provide a mechanism for the habituation effects reported previously in the SC (Boehnke et al. 2011; Woods and Frost 1977).

Effects of Visual Receptive Fields on Saccades

We investigated in detail how the sparse noise stimulus that was used to map the RFs influenced the latency of saccades. In the context of the monkeys' saccade task, the elements of the sparse noise stimulus are distractors, so that their effects may be comparable to those observed in previous studies of the effects of single distractors on the preparation and execution of saccades. One particularly well-studied distractor influence is the remote distractor effect: distractors presented far from the saccade target increase SRTs but do not change the saccade

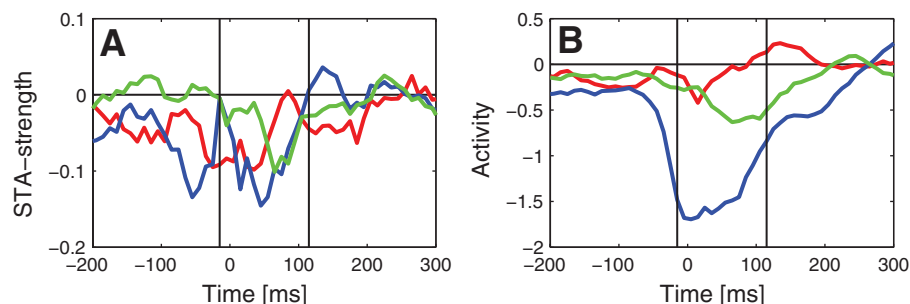


Fig. 9. A: normalized STA strength for the three classes of neurons around the time of ipsiversive saccades. Visuomotor neurons are marked as red lines, buildup neurons in blue, and visual neurons in green. Vertical black lines mark the area in which the strength of visual responses is likely to be underestimated since it is influenced by stimuli presented during the saccade. B: normalized spiking activity for the three classes of neurons.

vector (Edelman and Xu 2009; McSorley et al. 2012; Walker et al. 1997; Weber and Fischer 1994). In our data, we did not observe a remote distractor effect, presumably because the sparse noise stimulus always contained distractors at remote positions, so that the influence of remote distractors was approximately constant across saccades. In our data, the clearest effect of distractors on SRTs was found for stimuli flashed on the foveal side of the saccade target (Fig. 6). A similar result was obtained by Dorris et al. (2007), who reported asymmetries in saccades and related those to asymmetric influences of distractors on the firing rates of SC neurons. The asymmetry in the relative position of excitatory and suppressive RF regions found in our study (Fig. 4) may serve as the basis of these effects. In the time domain, we found a similar qualitative correspondence between the timing of inhibitory neuronal effects (Fig. 5) and the SRT delay associated with stimulation of the surrounds. Of course, neither our findings nor those of Dorris et al. (2007) prove that the SC is solely responsible for these behavioral results, as many other brain regions are involved in visual and oculomotor processing (Munoz 2002). In this regard, it would be interesting to determine whether neurons in these areas exhibit foveal biases similar to what we have reported here, and to what extent such biases are correlated with saccade behavior.

Although our results are generally consistent with the idea that distractor influences vary across space and time, there are important differences between our task and the tasks used in previous work (Godijn and Theeuwes 2002; McPeck and Keller 2001; McPeck et al. 2003; McSorley et al. 2006). In most previous studies, the subjects were engaged in a task (such as visual search) that required discriminating between the target and the distractor, such that the position of the saccade goal was not known before the presentation of the stimuli. In contrast, in our task the position of the saccade target was in most cases fully predictable, as the monkeys had to make several hundred identical leftward and rightward saccades during each session. Moreover, the distractors in our paradigm were very easy to distinguish, as they differed from the target along basic visual dimensions, such as luminance, color, duration, and size. Finally, in our paradigm many distractors were presented in parallel, and their position changed quickly over time, so that each single distractor would be expected to have very weak behavioral salience. Thus overall the distractors in our paradigm were easy to ignore and irrelevant to the task, so that our paradigm may be ideal for isolating the effects of bottom-up processing on visuomotor integration.

Effects of Saccades on Visual Receptive Fields

In our STA analyses, we defined the strength of the RF based on the correlation between the spikes and the visual stimuli. Thus it is not surprising that the STA strengths decreased around the time of saccades (Fig. 8), as the preparatory and motor activity found in the SC is by definition uncorrelated with the visual stimulus. However, we observed two consistent effects that could not be accounted for based on a purely linear model of the interactions between motor and visual signals. The first was an increase in the RF strength during the presaccadic period in many visuomotor and buildup neurons (Fig. 8, C and D). This increase was likely related to the presaccadic

increase in contrast sensitivity previously reported for the SC (Li and Basso 2008) and in the cortex (e.g., Martinez-Trujillo and Treue 2002), as well as the close link between shifts of attention and the initiation of saccades (Fischer and Breitmeyer 1987; Kustov and Robinson 1996; Mackeben and Nakayama 1993; Posner 1980). Indeed there is some evidence that attentional effects in the visual cortex may be caused in part by orienting responses originating in the SC (Muller et al. 2005; Wurtz and Goldberg 1972b).

The second effect of saccades on visual responses was a postsaccadic increase in STA strength that was especially prominent in the purely visual cells (Fig. 8E). A similar postsaccadic enhancement of visual responses has been observed in several cortical areas (Ibbotson et al. 2007, 2008); in the SC the enhancement may serve to facilitate the generation of short-latency corrective saccades (Cohen and Ross 1978).

Our data do not address the specific mechanisms underlying these nonlinearities. However, the results are generally inconsistent with a simple static nonlinearity applied to the firing rates of the neurons from which we recorded, as the same firing rates can be associated with different changes in STA strength, depending on the timing of the response relative to the saccade (e.g., Fig. 8E). Thus a more likely source of the nonlinear effects is a saccade-related change in contrast or response gain, as has been seen in the cortex (e.g., Ibbotson et al. 2007).

Relationship of Perisaccadic Effects to Visual Perception

Psychophysical studies have revealed a number of profound changes in visual perception that occur around the time of a saccade (Ross et al. 2001). These include changes in the perception of visual space (Honda 1989; Lappe et al. 2000; Matin and Pearce 1965; Richard et al. 2009; Ross et al. 1997) and overall visual sensitivity for certain stimuli (Bridgeman et al. 1975; Diamond et al. 2000; Holt 1903). The latter is known as saccadic suppression. Generally saccadic suppression is characterized by a time course in which visual sensitivity begins to decrease roughly 100 ms before a saccade, remains low during the saccade, and often increases immediately after a saccade (postsaccadic enhancement; Burr et al. 1994; Ibbotson et al. 2007, 2008; Kagan et al. 2008). A possible basis for these changes in sensitivity has been found in various cortical areas (Bremmer et al. 2009; Ibbotson et al. 2007; Ilg and Hoffmann 1993).

Although the neural substrate for these perceptual effects is presumably in the cortex (Bremmer et al. 2009; Ibbotson et al. 2008; Thiele et al. 2002), there is strong evidence that the corollary discharge signal that may serve as the basis of these effects has its origin in the SC (Sommer and Wurtz 2002, 2006; Wurtz et al. 2005). This hypothesis predicts that the time course of responses in the SC should resemble the time course of cortical changes in visual sensitivity. Consistent with this idea, our results (Fig. 8) show a similar time course in the strength of the STAs, particularly in visuomotor and buildup neurons. The suppression we have observed in the SC is generally associated with an increase in neuronal firing rates, whereas cortical suppression is typically associated with decreased responses to visual stimuli (Bremmer et al. 2009; Cloherty et al. 2010). These two ideas can be reconciled if the corollary discharge signal that reaches the cortex from the SC

(Sommer and Wurtz 2004a, b, 2006) ultimately exerts an inhibitory effect on visual responses, as suggested by various behavioral observations that saccadic suppression is associated with a reduction in the gain of visual inputs (Burr and Morrone 1996; Knoll et al. 2011; Watson and Krekelberg 2011). In the mouse and the rat, the process of suppressing visual sensitivity begins within the SC itself (Lee et al. 2007; Phongphanphanee et al. 2011), where cells in the intermediate layers exert polysynaptic inhibition over visual cells in the superficial layers. A similar mechanism may exist in the primate SC, which also contains a superficial layer that is predominantly visual and which projects indirectly to the visual cortex (Berman and Wurtz 2010, 2011).

Some behavioral studies have reported that saccadic suppression is followed by a postsaccadic enhancement of visual sensitivity (Burr et al. 1994; Knoll et al. 2011), and similar results have been found in cortical neurons (Ibbotson et al. 2007, 2008; Kagan et al. 2008). In the SC, our results indicate a consistent postsaccadic enhancement of STA strength, particularly in visual neurons. For these cells, the pattern of perisaccadic effects was most similar to that observed in the LGN (Reppas et al. 2002), with strong enhancement following weak suppression. This enhancement may result from increases in the efficacy of retinogeniculate transmission, which in turn appear to result from perisaccadic changes in brain stem modulatory inputs (Singer and Bedworth 1974). Further analysis of our SC data suggests that, in contrast to the suppression effects described above, the enhancement effects were associated with a decrease in firing rate. Thus the SC exhibits a pattern of perisaccadic effects similar to that observed behaviorally, with the relationship between firing rate and visual sensitivity being opposite that found in the cortex.

Although there is a clear symmetry in the changes in firing rates and the changes in STA strength, it is likely that the suppression and enhancement of the STA are mediated by different mechanisms. For suppression, the mechanism can for the most part be understood in a straightforward way as a decorrelation of the visual input from the spike train via the introduction of spikes related to the initiation of the saccade (Fig. 8). In contrast, perisaccadic changes in firing rate are by themselves insufficient to explain postsaccadic enhancement: decreases in firing rate found before a saccade or around the time of an ipsiversive saccade yield little change in STA strength. Moreover, the strongest enhancement is found in cells that exhibit no discernible motor activity around the time of a saccade (visual cells; Fig. 8), suggesting that there is no straightforward way to relate changes in the STA strength to changes in the motor activity in the same cells. Rather postsaccadic enhancement may be mediated by a transient withdrawal of a tonic source of nonvisual inputs to the SC. This would account for the stronger correlation between visual responses and spiking activity and its relationship to changes in firing rate (Fig. 8E).

ACKNOWLEDGMENTS

We thank Julie Coursol and Cathy Hunt for technical assistance.

GRANTS

This work was supported by a Canadian Institutes of Health Research grant to D. Guitton (MOP-9222) and by grants from National Sciences and Engineering Research Council (341534-12) and The EJLB Foundation to C. C. Pack.

DISCLOSURES

No conflicts of interest, financial or otherwise, are declared by the author(s).

AUTHOR CONTRIBUTIONS

Author contributions: J.C., D.G., and C.C.P. conception and design of research; J.C. performed experiments; J.C. and C.C.P. analyzed data; J.C., D.G., and C.C.P. interpreted results of experiments; J.C. prepared figures; J.C. drafted manuscript; J.C., D.G., and C.C.P. edited and revised manuscript; J.C., D.G., and C.C.P. approved final version of manuscript.

REFERENCES

- Barlow HB, Fitzhugh R, Kuffler SW. Change of organization in the receptive fields of the cat's retina during dark adaptation. *J Physiol* 137: 338–354, 1957.
- Basso MA, Wurtz RH. Modulation of neuronal activity by target uncertainty. *Nature* 389: 66–69, 1997.
- Berman RA, Wurtz RH. Functional identification of a pulvinar path from superior colliculus to cortical area MT. *J Neurosci* 30: 6342–6354, 2010.
- Berman RA, Wurtz RH. Signals conveyed in the pulvinar pathway from superior colliculus to cortical area MT. *J Neurosci* 31: 373–384, 2011.
- Boehne SE, Berg DJ, Marino RA, Baldi PF, Itti L, Munoz DP. Visual adaptation and novelty responses in the superior colliculus. *Eur J Neurosci* 34: 766–779, 2011.
- Boehne SE, Munoz DP. On the importance of the transient visual response in the superior colliculus. *Curr Opin Neurobiol* 18: 544–551, 2008.
- Brainard DH. The psychophysics toolbox. *Spat Vis* 10: 433–436, 1997.
- Bremner F, Kubischik M, Hoffmann KP, Krekelberg B. Neural dynamics of saccadic suppression. *J Neurosci* 29: 12374–12383, 2009.
- Bridgeman B, Hendry D, Stark L. Failure to detect displacement of the visual world during saccadic eye movements. *Vision Res* 15: 719–722, 1975.
- Burr DC, Morgan MJ, Morrone MC. Saccadic suppression precedes visual motion analysis. *Curr Biol* 9: 1207–1209, 1999.
- Burr DC, Morrone MC. Temporal impulse response functions for luminance and colour during saccades. *Vision Res* 36: 2069–2078, 1996.
- Burr DC, Morrone MC, Ross J. Selective suppression of the magnocellular visual pathway during saccadic eye movements. *Nature* 371: 511–513, 1994.
- Choi WY, Guitton D. Responses of collicular fixation neurons to gaze shift perturbations in head-unrestrained monkey reveal gaze feedback control. *Neuron* 50: 491–505, 2006.
- Churan J, Guitton D, Pack CC. Context dependence of receptive field remapping in superior colliculus. *J Neurophysiol* 106: 1862–1874, 2011.
- Cloherty SL, Mustari MJ, Rosa MG, Ibbotson MR. Effects of saccades on visual processing in primate MSTd. *Vision Res* 50: 2683–2691, 2010.
- Cohen ME, Ross LE. Latency and accuracy characteristics of saccades and corrective saccades in children and adults. *J Exp Child Psychol* 26: 517–527, 1978.
- Cynader M, Berman N. Receptive-field organization of monkey superior colliculus. *J Neurophysiol* 35: 187–201, 1972.
- Diamond MR, Ross J, Morrone MC. Extraretinal control of saccadic suppression. *J Neurosci* 20: 3449–3455, 2000.
- Dorris MC, Munoz DP. Saccadic probability influences motor preparation signals and time to saccadic initiation. *J Neurosci* 18: 7015–7026, 1998.
- Dorris MC, Olivier E, Munoz DP. Competitive integration of visual and preparatory signals in the superior colliculus during saccadic programming. *J Neurosci* 27: 5053–5062, 2007.
- Dunn CA, Hall NJ, Colby CL. Spatial updating in monkey superior colliculus in the absence of the forebrain commissures: dissociation between superficial and intermediate layers. *J Neurophysiol* 104: 1267–1285, 2010.
- Edelman JA, Xu KZ. Inhibition of voluntary saccadic eye movement commands by abrupt visual onsets. *J Neurophysiol* 101: 1222–1234, 2009.
- Fischer B, Breitmeyer B. Mechanisms of visual attention revealed by saccadic eye movements. *Neuropsychologia* 25: 73–83, 1987.

- Godijn R, Theeuwes J.** Programming of endogenous and exogenous saccades: evidence for a competitive integration model. *J Exp Psychol Hum Percept Perform* 28: 1039–1054, 2002.
- Goldberg ME, Wurtz RH.** Activity of superior colliculus in behaving monkey. I. Visual receptive fields of single neurons. *J Neurophysiol* 35: 542–559, 1972.
- Guitton D, Crommelinck M, Roucoux A.** Stimulation of the superior colliculus in the alert cat. I. Eye movements and neck EMG activity evoked when the head is restrained. *Exp Brain Res* 39: 63–73, 1980.
- Harutiunian-Kozak B, Dec K, Wrobel A.** The organization of visual receptive fields of neurons in the cat colliculus superior. *Acta Neurobiol Exp (Warsz)* 33: 563–573, 1973.
- Holt E.** Eye movement and central anesthesia. *Harvard Psychological Studies* 1: 3–45, 1903.
- Honda H.** Perceptual localization of visual stimuli flashed during saccades. *Percept Psychophys* 45: 162–174, 1989.
- Humphrey NK.** Responses to visual stimuli of units in the superior colliculus of rats and monkeys. *Exp Neurol* 20: 312–340, 1968.
- Ibbotson M, Krekelberg B.** Visual perception and saccadic eye movements. *Curr Opin Neurobiol* 21: 553–558, 2011.
- Ibbotson MR, Crowder NA, Cloherty SL, Price NS, Mustari MJ.** Saccadic modulation of neural responses: possible roles in saccadic suppression, enhancement, and time compression. *J Neurosci* 28: 10952–10960, 2008.
- Ibbotson MR, Price NS, Crowder NA, Ono S, Mustari MJ.** Enhanced motion sensitivity follows saccadic suppression in the superior temporal sulcus of the macaque cortex. *Cereb Cortex* 17: 1129–1138, 2007.
- Ichida JM, Schwabe L, Bressloff PC, Angelucci A.** Response facilitation from the “suppressive” receptive field surround of macaque V1 neurons. *J Neurophysiol* 98: 2168–2181, 2007.
- Ilg UJ, Hoffmann KP.** Motion perception during saccades. *Vision Res* 33: 211–220, 1993.
- Jones JP, Palmer LA.** The two-dimensional spatial structure of simple receptive fields in cat striate cortex. *J Neurophysiol* 58: 1187–1211, 1987.
- Kagan I, Gur M, Snodderly DM.** Saccades and drifts differentially modulate neuronal activity in V1: effects of retinal image motion, position, and extraretinal influences. *J Vis* 8: 19.1.251187–19, 2008.
- Knoll J, Binda P, Morrone MC, Bremmer F.** Spatiotemporal profile of peri-saccadic contrast sensitivity. *J Vis* 11: 15, 2011.
- Kustov AA, Robinson DL.** Shared neural control of attentional shifts and eye movements. *Nature* 384: 74–77, 1996.
- Lappe M, Awater H, Krekelberg B.** Postsaccadic visual references generate presaccadic compression of space. *Nature* 403: 892–895, 2000.
- Lee C, Lee J.** Visual motion perception at the time of saccadic eye movements and its relation to spatial mislocalization. *Ann N Y Acad Sci* 1039: 160–165, 2005.
- Lee PH, Sooksawat T, Yanagawa Y, Isa K, Isa T, Hall WC.** Identity of a pathway for saccadic suppression. *Proc Natl Acad Sci U S A* 104: 6824–6827, 2007.
- Li X, Basso MA.** Preparing to move increases the sensitivity of superior colliculus neurons. *J Neurosci* 28: 4561–4577, 2008.
- Livingstone MS, Pack CC, Born RT.** Two-dimensional substructure of MT receptive fields. *Neuron* 30: 781–793, 2001.
- Mackeben M, Nakayama K.** Express attentional shifts. *Vision Res* 33: 85–90, 1993.
- Marino RA, Rodgers CK, Levy R, Munoz DP.** Spatial relationships of visuomotor transformations in the superior colliculus map. *J Neurophysiol* 100: 2564–2576, 2008.
- Marrocco RT, Li RH.** Monkey superior colliculus: properties of single cells and their afferent inputs. *J Neurophysiol* 40: 844–860, 1977.
- Martinez-Trujillo J, Treue S.** Attentional modulation strength in cortical area MT depends on stimulus contrast. *Neuron* 35: 365–370, 2002.
- Matin L, Pearce DG.** Visual perception of direction for stimuli flashed during voluntary saccadic eye movements. *Science* 148: 1485–1488, 1965.
- Mays LE, Sparks DL.** Saccades are spatially, not retinocentrically, coded. *Science* 208: 1163–1165, 1980.
- McPeck RM.** Reversal of a distractor effect on saccade target selection after superior colliculus inactivation. *J Neurophysiol* 99: 2694–2702, 2008.
- McPeck RM, Han JH, Keller EL.** Competition between saccade goals in the superior colliculus produces saccade curvature. *J Neurophysiol* 89: 2577–2590, 2003.
- McPeck RM, Keller EL.** Deficits in saccade target selection after inactivation of superior colliculus. *Nat Neurosci* 7: 757–763, 2004.
- McPeck RM, Keller EL.** Short-term priming, concurrent processing, and saccade curvature during a target selection task in the monkey. *Vision Res* 41: 785–800, 2001.
- McSorley E, Haggard P, Walker R.** Time course of oculomotor inhibition revealed by saccade trajectory modulation. *J Neurophysiol* 96: 1420–1424, 2006.
- McSorley E, McCloy R, Lyne C.** The spatial impact of visual distractors on saccade latency. *Vision Res* 60: 61–72, 2012.
- Muller JR, Philiastides MG, Newsome WT.** Microstimulation of the superior colliculus focuses attention without moving the eyes. *Proc Natl Acad Sci U S A* 102: 524–529, 2005.
- Munoz DP.** Commentary: saccadic eye movements: overview of neural circuitry. *Prog Brain Res* 140: 89–96, 2002.
- Nummela SU, Krauzlis RJ.** Inactivation of primate superior colliculus biases target choice for smooth pursuit, saccades, and button press responses. *J Neurophysiol* 104: 1538–1548, 2010.
- Pack CC, Conway BR, Born RT, Livingstone MS.** Spatiotemporal structure of nonlinear subunits in macaque visual cortex. *J Neurosci* 26: 893–907, 2006.
- Pelli DG.** The VideoToolbox software for visual psychophysics: transforming numbers into movies. *Spat Vis* 10: 437–442, 1997.
- Phongphanphane P, Mizuno F, Lee PH, Yanagawa Y, Isa T, Hall WC.** A circuit model for saccadic suppression in the superior colliculus. *J Neurosci* 31: 1949–1954, 2011.
- Platt B, Withington DJ.** Response habituation in the superficial layers of the guinea-pig superior colliculus in vitro. *Neurosci Lett* 221: 153–156, 1997.
- Posner MI.** Orienting of attention. *Q J Exp Psychol B* 32: 3–25, 1980.
- Reppas JB, Usrey WM, Reid RC.** Saccadic eye movements modulate visual responses in the lateral geniculate nucleus. *Neuron* 35: 961–974, 2002.
- Richard A, Churan J, Guitton DE, Pack CC.** The geometry of perisaccadic visual perception. *J Neurosci* 29: 10160–10170, 2009.
- Ringach DL, Shapley D.** Reverse correlation in neurophysiology. *Cogn Sci* 28: 147–166, 2004.
- Robinson DA.** A method of measuring eye movement using a scleral search coil in a magnetic field. *IEEE Trans Biomed Eng* 10: 137–145, 1963.
- Ross J, Morrone MC, Burr DC.** Compression of visual space before saccades. *Nature* 386: 598–601, 1997.
- Ross J, Morrone MC, Goldberg ME, Burr DC.** Changes in visual perception at the time of saccades. *Trends Neurosci* 24: 113–121, 2001.
- Sceniak MP, Ringach DL, Hawken MJ, Shapley R.** Contrast’s effect on spatial summation by macaque V1 neurons. *Nat Neurosci* 2: 733–739, 1999.
- Singer W, Bedworth N.** Correlation between the effects of brain stem stimulation and saccadic eye movements on transmission in the cat lateral geniculate nucleus. *Brain Res* 72: 185–202, 1974.
- Sommer MA, Wurtz RH.** Influence of the thalamus on spatial visual processing in frontal cortex. *Nature* 444: 374–377, 2006.
- Sommer MA, Wurtz RH.** A pathway in primate brain for internal monitoring of movements. *Science* 296: 1480–1482, 2002.
- Sommer MA, Wurtz RH.** Visual perception and corollary discharge. *Perception* 37: 408–418, 2008.
- Sommer MA, Wurtz RH.** What the brain stem tells the frontal cortex. I. Oculomotor signals sent from superior colliculus to frontal eye field via mediodorsal thalamus. *J Neurophysiol* 91: 1381–1402, 2004.
- Sommer MA, Wurtz RH.** What the brain stem tells the frontal cortex. II. Role of the SC-MD-FEF pathway in corollary discharge. *J Neurophysiol* 91: 1403–1423, 2004.
- Sparks DL, Nelson JS.** Sensory and motor maps in the mammalian superior colliculus. *Trends Neurosci* 10: 312–317, 1987.
- Sperry RW.** Neural basis of the spontaneous optokinetic response produced by visual inversion. *J Comp Physiol Psychol* 43: 482–489, 1950.
- Szulborski RG, Palmer LA.** The two-dimensional spatial structure of nonlinear subunits in the receptive fields of complex cells. *Vision Res* 30: 249–254, 1990.
- Thiele A, Henning P, Kubischik M, Hoffmann KP.** Neural mechanisms of saccadic suppression. *Science* 295: 2460–2462, 2002.
- Tsui JM, Pack CC.** Contrast sensitivity of MT receptive field centers and surrounds. *J Neurophysiol* 106: 1888–1900, 2011.
- Updyke BV.** Characteristics of unit responses in superior colliculus of the Cebus monkey. *J Neurophysiol* 37: 896–909, 1974.
- van Watter SM, van Opstal AJ.** Perisaccadic mislocalization of visual targets by head-free gaze shifts: visual or motor? *J Neurophysiol* 100: 1848–1867, 2008.
- von Holst E, Mittelstaedt H.** Das Refferenzprinzip. *Naturwissenschaften* 37: 464–476, 1950.

- Walker MF, Fitzgibbon EJ, Goldberg ME.** Neurons in the monkey superior colliculus predict the visual result of impending saccadic eye movements. *J Neurophysiol* 73: 1988–2003, 1995.
- Walker R, Deubel H, Schneider WX, Findlay JM.** Effect of remote distractors on saccade programming: evidence for an extended fixation zone. *J Neurophysiol* 78: 1108–1119, 1997.
- Watson T, Krekelberg B.** An equivalent noise investigation of saccadic suppression. *J Neurosci* 31: 6535–6541, 2011.
- Weber H, Fischer B.** Differential effects of non-target stimuli on the occurrence of express saccades in man. *Vision Res* 34: 1883–1891, 1994.
- Woods EJ, Frost BJ.** Adaptation and habituation characteristics of tectal neurons in the pigeon. *Exp Brain Res* 27: 347–354, 1977.
- Wurtz RH.** Neuronal mechanisms of visual stability. *Vision Res* 48: 2070–2089, 2008.
- Wurtz RH, Goldberg ME.** Activity of superior colliculus in behaving monkey. 3. Cells discharging before eye movements. *J Neurophysiol* 35: 575–586, 1972.
- Wurtz RH, Goldberg ME.** The primate superior colliculus and the shift of visual attention. *Invest Ophthalmol* 11: 441–450, 1972.
- Wurtz RH, Goldberg ME.** Superior colliculus cell responses related to eye movements in awake monkeys. *Science* 171: 82–84, 1971.
- Wurtz RH, Sommer MA, Cavanaugh J.** Drivers from the deep: the contribution of collicular input to thalamocortical processing. *Prog Brain Res* 149: 207–225, 2005.

